

Sources of Electrical Conductivity in SnO<sub>2</sub>Abhishek Kumar Singh,<sup>1</sup> Anderson Janotti,<sup>1</sup> Matthias Scheffler,<sup>1,2</sup> and Chris G. Van de Walle<sup>1</sup><sup>1</sup>Materials Department, University of California, Santa Barbara, California 93106, USA<sup>2</sup>Fritz-Haber-Institut der Max-Planck-Gesellschaft, Faradayweg 4-6, D-14195 Berlin, Germany

(Received 19 July 2007; published 31 July 2008)

SnO<sub>2</sub> is widely used as a transparent conductor and sensor material. Better understanding and control of its conductivity would enhance its performance in existing applications and enable new ones, such as in light emitters. Using density functional theory, we show that the conventional attribution of *n*-type conductivity to intrinsic point defects is incorrect. Unintentional incorporation of hydrogen provides a consistent explanation of experimental observations. Most importantly, we find that SnO<sub>2</sub> offers excellent prospects for *p*-type doping by incorporation of acceptors on the Sn site. Specific strategies for optimizing acceptor incorporation are presented.

DOI: 10.1103/PhysRevLett.101.055502

PACS numbers: 61.72.Bb, 61.72.J-, 68.55.Ln

Wide-band-gap oxides hold great promise for applications as semiconductors, but progress has been impeded by the lack of control over conductivity [1,2]. Unipolar doping (e.g., *n*-type) suffices for some purposes, such as transparent conductors or field effect transistors [1]. Ambipolar doping would enable an entire additional range of devices, including optical detectors and light emitters [2]. Indeed, the availability of bulk single-crystal substrates would give the oxides an edge over the III-nitrides. However, controlling the *n*-type conductivity and achieving reproducible *p*-type doping still poses serious challenges. Most of the wide-band-gap oxides exhibit unintentional *n*-type conductivity, whose cause is still widely debated [1,2].

SnO<sub>2</sub> has a direct band gap of 3.6 eV and is widely used as a transparent conductor and in gas sensors [3,4]. As-grown SnO<sub>2</sub> generally exhibits high levels of unintentional *n*-type conductivity [5–8]. Because this conductivity varies inversely with the oxygen partial pressure, it has been commonly attributed to the presence of native point defects, in particular, to oxygen vacancies [3,5–7]. However, to our knowledge, no direct experimental observations of oxygen vacancies or their relation to the electrical conductivity have been reported.

Relying on calculations based on density functional theory in the local-density approximation (DFT-LDA), Kiliç and Zunger [9] concluded that Sn interstitials (Sn<sub>i</sub>) and oxygen vacancies (V<sub>O</sub>) are the cause of unintentional *n*-type conductivity in SnO<sub>2</sub>. However, we feel that their conclusions are unwarranted because they were based on a forthright application of DFT-LDA. It is well known that DFT-LDA severely underestimates band gaps and can lead to large errors in formation energies and position of electronic transition levels of point defects and impurities, especially in wide-band-gap semiconductors [10].

Based on a method that goes beyond the LDA, we investigate the role of point defects and hydrogen on the unintentional *n*-type conductivity and the possibility of *p*-type doping in SnO<sub>2</sub>. We find that (i) intrinsic point defects, such as V<sub>O</sub> and Sn<sub>i</sub>, are unlikely to be the cause of *n*-type conductivity in as-grown or annealed SnO<sub>2</sub>, and

(ii) instead, this conductivity can be explained by inadvertent incorporation of impurities, in particular, hydrogen, which is generally difficult to detect but very likely to be present in the growth and/or processing environments. Besides incorporating on interstitial sites, hydrogen can also replace oxygen in SnO<sub>2</sub> and form a multicenter bond with its three Sn nearest neighbors [11]. Substitutional hydrogen has a low formation energy, acts as a shallow donor, and consistently explains experimental observations [12–14]. (iii) *p*-type doping in SnO<sub>2</sub> has a significantly higher chance of success than in other oxides such as ZnO. We find that incorporation of group-IIIa atoms (In, Ga, and Al) on the Sn site produces shallow acceptors that exhibit good solubility and a low degree of self-compensation. We also provide specific prescriptions for suppressing compensation by intrinsic point defects.

Our calculations are based on density functional theory within the generalized gradient approximation (GGA). The semicore Sn *d* states in SnO<sub>2</sub> are explicitly treated as valence states through the projector augmented wave method as implemented in the VASP code [15–18]. Unfortunately, GGA (as well as LDA) underestimates the binding energy of these *d* states and severely affects the band gap, beyond the typical GGA (or LDA) underestimation. In order to correct the position of the *d* states, we include an on-site Coulomb correlation interaction as given by the GGA + *U* method. This improves the description of semicore states and, by indirectly affecting the Sn *d*-O *p* coupling and the Sn *s* states, leads to larger band gaps [19,20]. It also significantly improves the description of deformation potentials and band offsets in oxides and nitrides [19,20]. The value of *U* was determined by calculating *U* for the atom and screening this value by using the high-frequency dielectric constant  $\epsilon^\infty$  of the solid [21]. For SnO<sub>2</sub>, this approach results in *U* = 3.5 eV for Sn *d* states. The calculated band gaps using GGA and GGA + *U* are 0.95 and 1.65 eV, respectively, compared to the experimental value of 3.60 eV.

Point defects and impurities are simulated using 216-atom supercells, a 2 × 2 × 2 mesh of Monkhorst-Pack

points for integrations over the Brillouin zone [22], and a 400 eV cutoff in the plane-wave expansions. All calculations are performed at the theoretical equilibrium lattice parameters of the rutile structure, which are within 1% of the experimental values ( $a = 4.73 \text{ \AA}$  and  $c = 3.18 \text{ \AA}$ ) [23].

The formation energy of a point defect or impurity is a key quantity that determines its equilibrium concentration; high formation energies imply low concentrations. The formation energy of a point defect  $D$  in charge state  $q$  is given by [24]

$$E^f(D^q) = E_{\text{tot}}(D^q) - E_{\text{tot}}(\text{SnO}_2) - n_{\text{O}}[\mu_{\text{O}} + \frac{1}{2}E_{\text{tot}}(\text{O}_2)] - n_{\text{Sn}}[\mu_{\text{Sn}} + E_{\text{tot}}(\text{Sn}^0)] + q(E_F + E_v + \Delta V), \quad (1)$$

where  $E_{\text{tot}}(D^q)$  is the total energy of the supercell containing the defect in charge state  $q$ , and  $E_{\text{tot}}(\text{SnO}_2)$  is the total energy of the perfect crystal in the same supercell.  $E_F$  is the Fermi level, referenced to the valence-band maximum (VBM)  $E_v$ , and  $\Delta V$  aligns the VBM in the defect and perfect crystal supercells [24]. The quantities  $n_{\text{O}}$  and  $n_{\text{Sn}}$  are the number of O and Sn atoms, respectively, that have been added (or removed) to form the defect. The chemical potentials  $\mu_{\text{O}}$  and  $\mu_{\text{Sn}}$  are referenced to the calculated total energies of O in  $\text{O}_2$  molecules [ $\frac{1}{2}E_{\text{tot}}(\text{O}_2)$ ] and Sn in  $\alpha\text{-Sn}$  [ $E_{\text{tot}}(\text{Sn}^0)$ ], respectively. They are subject to upper bounds  $\mu_{\text{O}} \leq 0$  (O-rich limit) and  $\mu_{\text{Sn}} \leq 0$  (Sn-rich limit) and must satisfy the stability condition of  $\text{SnO}_2$ :  $\mu_{\text{Sn}} + 2\mu_{\text{O}} = \Delta H_f(\text{SnO}_2)$ , where  $\Delta H_f(\text{SnO}_2)$  is the enthalpy of formation of  $\text{SnO}_2$ . We obtain  $\Delta H_f(\text{SnO}_2) = -5.21 \text{ eV}$  (GGA) and  $-6.03 \text{ eV}$  (GGA +  $U$ ), the latter in better agreement with the experimental value of  $-5.98 \text{ eV}$  [25]. In addition, we have examined  $\text{SnO}$  and  $\text{H}_2\text{O}$  as limiting phases and found that these do not affect our conclusions.

From formation energies  $E^f(D^q)$ , we can extract transition levels  $\varepsilon(q/q')$ , i.e., the Fermi-level positions at which the defect changes charge state. Since DFT-GGA severely underestimates band gaps, a correction is required in order to compare transition levels and formation energies with experimental results. Here we use GGA and GGA +  $U$  results to extrapolate transition levels and formation energies to the experimental gap, following a procedure described in Ref. [21]. This approach has been successfully applied to native defects in  $\text{ZnO}$ , producing results that agree with experiment [10,19].

In the case of the oxygen vacancy, the transition level  $\varepsilon(2+/0)$  is located at 1.24 eV above the VBM in GGA and at 1.39 eV in GGA +  $U$ ; the extrapolated value is 1.80 eV. This result clearly shows that  $V_{\text{O}}$  is a deep donor, with an ionization energy of  $\sim 1.8 \text{ eV}$ . Oxygen vacancies therefore *cannot* be the origin of  $n$ -type conductivity in  $\text{SnO}_2$ . Figure 1(a) shows the formation energies of  $V_{\text{O}}$ ,  $\text{Sn}_i$ , and  $\text{Sn}_{\text{O}}$  (the tin antisite) as a function of  $E_F$  in the Sn-rich limit (which is most favorable for formation of these defects). For  $E_F$  near the VBM,  $V_{\text{O}}$  is stable in the 2+ charge state and, therefore, can act as a compensating

center for  $p$ -type conductivity. In  $n$ -type  $\text{SnO}_2$ , where  $E_F$  is near the conduction-band minimum,  $V_{\text{O}}$  is stable in the neutral charge state. The 1+ charge state is unstable for all values of  $E_F$  in the band gap. The origin of this “negative- $U$ ” behavior lies in the large differences in local lattice relaxations for different charge states. For  $V_{\text{O}}^0$  the three nearest-neighbor Sn atoms relax inward by 2.5%, while for  $V_{\text{O}}^+$  and  $V_{\text{O}}^{2+}$  the relaxations are outward by 5.6% and 10% of the equilibrium Sn-O bond length, respectively [see Fig. 2(a)].

The Sn interstitial [Fig. 2(b)] acts as a shallow donor, being stable exclusively in the 4+ charge state. However, its formation energy in  $n$ -type material is exceedingly high (12 eV), indicating that the concentration of  $\text{Sn}_i$  will be negligibly low under equilibrium conditions. Note that we find the 3+ and 2+ charge states of  $\text{Sn}_i$  to be unstable; we believe that the results reported in Ref. [9] correspond to an erroneous occupation of extended bulk states instead of defect-related states. In order to explore the stability of  $\text{Sn}_i^{4+}$ , we have also calculated its migration barrier.  $\text{Sn}_i^{4+}$  migrates through the interstitial channels along the [001] direction with an energy barrier of 0.43 eV; this very low barrier implies that the Sn interstitial is highly mobile even below room temperature. Therefore, it is unlikely that Sn interstitials will be present in nonequilibrium concentrations. The combination of equilibrium and kinetic results allows us to conclude that  $\text{Sn}_i$  cannot be the cause of unintentional  $n$ -type conductivity in  $\text{SnO}_2$ , either.

The third donor-type defect  $\text{Sn}_{\text{O}}$  is similar to  $\text{Sn}_i$ ; it acts as a shallow donor, being stable only in the 4+ charge state [Fig. 1(a)], but it also has an extremely high formation energy in  $n$ -type  $\text{SnO}_2$ , implying a negligibly low equilibrium concentration. Nonequilibrium incorporation of  $\text{Sn}_{\text{O}}$  could occur, for instance, due to implantation or electron irradiation but is highly unlikely to occur during growth.

Since native point defects cannot explain the observed unintentional  $n$ -type doping, we explore other potential sources of conductivity. A number of impurities, such as

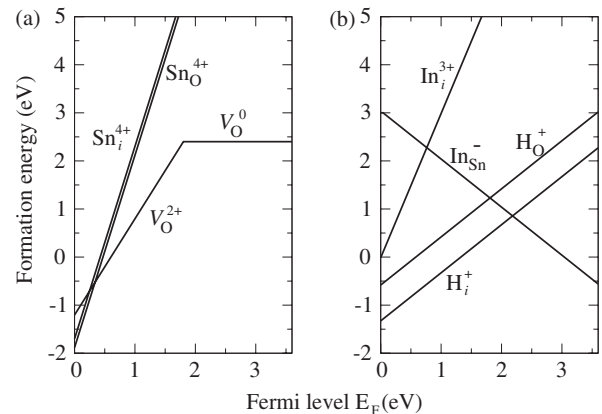


FIG. 1. Calculated formation energies of (a) intrinsic donor-type defects and (b) impurities in  $\text{SnO}_2$ , as a function of the Fermi level (referenced to the valence-band maximum), for Sn-rich conditions.

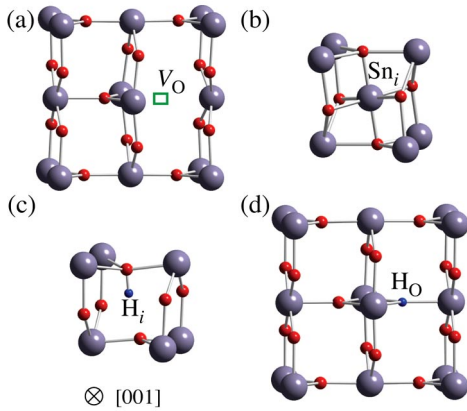


FIG. 2 (color online). Local structural configurations of (a)  $V_O^{2+}$ , (b)  $Sn_i^{4+}$ , (c)  $H_i^+$ , and (d)  $H_O^+$  in  $SnO_2$ .

F on an O site or Sb on a Sn site, are known to act as shallow donors in  $SnO_2$  [26–28]. However, as-grown  $SnO_2$  exhibits  $n$ -type conductivity even when not intentionally doped [5–8]. We therefore focus specifically on hydrogen, which is commonly present in (and difficult to exclude from) the various growth and processing environments.

We find that hydrogen can be incorporated on interstitial sites as well as on substitutional oxygen sites in  $SnO_2$ . Interstitial hydrogen ( $H_i$ ) forms a strong bond with an oxygen atom with an O-H bond length of 1.04 Å [Fig. 2(c)], slightly longer than the calculated bond length in  $H_2O$  (0.94 Å). It has low formation energy and acts as a shallow donor, as shown in Fig. 1(b). Interstitial hydrogen is therefore a plausible cause of  $n$ -type conductivity, as suggested in Ref. [29]. However, we find that  $H_i$  is highly mobile. Its migration path involves breaking the O-H bond and forming a new O-H bond with a nearest-neighbor O atom. The calculated migration energy barrier is as low as 0.57 eV, implying that  $H_i$  is mobile even below room temperature. Although additional barriers may be involved in removing  $H_i$  from the samples or neutralizing its electrical activity, the high mobility of  $H_i$  at relatively low temperatures indicates that it is unlikely to be the primary unintentional donor, contrary to previous suggestions [6,29]. Importantly, the observed dependence of conductivity on oxygen partial pressure [6] cannot be explained by invoking  $H_i$ , since its formation energy does not depend on  $\mu_O$ .

Hydrogen can also occupy oxygen sites ( $H_O$ ) in  $SnO_2$ , as shown in Fig. 2(d).  $H_O$  is threefold coordinated and forms a multicenter bond with its three nearest-neighbor Sn atoms [11]. The calculated Sn-H distance ( $\sim 2.14$  Å) is close to the equilibrium Sn-O bond length of 2.07 Å.  $H_O$  acts as a shallow donor, and its formation energy is only slightly higher than that of  $H_i$ , as shown in Fig. 1(b). Most importantly, since  $H_O$  involves removing an O atom from its lattice, its formation energy explicitly depends on the oxygen chemical potential  $\mu_O$ .  $H_O$  therefore provides a consistent explanation for the unintentional  $n$ -type conductivity in  $SnO_2$  and its variation with oxygen partial pressure [6,7].

Once formed, substitutional  $H_O$  is significantly more stable than  $H_i$ . The calculated binding energy of  $H_O^+$  with respect to  $V_O^0$  and  $H_i^+$  is 1.67 eV. The energy barrier for the dissociation of  $H_O^+$  into  $V_O^0$  and  $H_i^+$  is therefore 2.24 eV, estimated as the sum of the binding energy (1.67 eV) and the migration barrier of  $H_i^+$  (0.57 eV). We have also calculated the migration of  $H_O^+$  through a mechanism involving a concerted exchange with one of the neighboring oxygen atoms. The calculated barrier in this case is 2.2 eV. We conclude that  $H_O$  is stable enough to explain the observed unintentional  $n$ -type conductivity in  $SnO_2$  [5,8]. Indeed, an increase in carrier concentration has been observed upon exposure to moist air or  $H_2$  [12,13]. Nola *et al.* [13] also reported a decrease in the number of donors upon annealing at 573 K, consistent with our calculated barrier of  $\sim 2.2$  eV for the motion of  $H_O^+$ .

Having provided a better understanding of  $n$ -type conductivity, we now explore the potential for  $p$ -type doping in  $SnO_2$ . Conventionally we look for impurities with one fewer electron than Sn or O, i.e., impurities from group III or group V of the periodic table. We anticipate that doping with group-V acceptors will be difficult to achieve, since the VBM is composed mostly of O  $p$  states, and all group-V elements, including N, have significantly lower electronegativity than O. Group-V elements are therefore expected to give rise to deep acceptor levels. Indeed, our calculated ionization energy for  $N_O$  is 0.6 eV.

Doping with group-IIIA elements on the Sn site is a much more promising route to achieving  $p$ -type conductivity in  $SnO_2$ . Doping on the cation site also offers a notable advantage over other wide-band-gap semiconductors, such as ZnO. Acceptors substituting on the cation site in ZnO belong to group I of the periodic table. In group IA, Li, Na, and K are deep acceptors and/or show strong tendency for self-compensation due to concurrent incorporation on interstitial sites where they act as donors [30]. In group IB, Cu and Ag are deep acceptors due to the strong coupling between their shallow  $d$  states and the oxygen  $p$  states that compose the VBM [31]. In contrast, we find that elements from group IIIA (In, Ga, and Al) or group IIB (Zn) exhibit a distinct preference for incorporation on Sn sites and act as shallow acceptors in  $SnO_2$ .

Figure 1(b) shows the calculated formation energy of  $In_{Sn}$  under Sn-rich conditions (least favorable for In incorporation on the Sn site). The chemical potential  $\mu_{In}$  is limited by the formation of  $In_2O_3$  as a secondary phase, i.e.,  $2\mu_{In} + 3\mu_O \leq \Delta H_f(In_2O_3)$ . The calculated formation energies for  $Ga_{Sn}$  and  $Al_{Sn}$  (not shown) differ by less than 0.1 eV from those of  $In_{Sn}$ .  $Zn_{Sn}$  acts as a double acceptor, but its formation energy at  $E_F = 0$  is significantly higher. The calculated ionization energies given by the  $\varepsilon(0/-)$  transition levels [24] are about 100 meV, indicating that these impurities indeed act as effective-mass shallow acceptors. The formation energies of  $In_{Sn}$ ,  $Ga_{Sn}$ , and  $Al_{Sn}$  are significantly lower under Sn-poor conditions,

indicating that group-III A acceptors can be readily incorporated during growth.

We have also investigated two potential mechanisms for self-compensation of group-III A acceptors in  $\text{SnO}_2$ : incorporation on interstitial sites as donors and the possible formation of AX centers in which the impurity induces a large relaxation and becomes more stable in the positive charge state [30,32]. Figure 1(b) shows that indium interstitials ( $\text{In}_i$ ) have low formation energies in  $p$ -type  $\text{SnO}_2$ . However, this figure represents a worst-case scenario for the incorporation of acceptors on the Sn site, since it assumes extreme Sn-rich conditions. Moving away from the Sn-rich limit lowers the formation energy of substitutional acceptors relative to the formation energy of interstitial donors; it also significantly raises the formation energy of compensating point defects, such as  $V_{\text{O}}$ ,  $\text{Sn}_i$ , and  $\text{Sn}_{\text{O}}$ . This is strikingly different from the behavior of group-I acceptors in ZnO, where the interstitial donors tend to have lower formation energies than the substitutional acceptors even under Zn-poor conditions [30]. We also find that AX centers are unstable in  $\text{SnO}_2$ . The most likely configuration is one in which the acceptor would induce two neighboring O atoms to strongly relax toward each other and form an O-O bond by breaking two Sn-O bonds [30,32]. However, we find that the O atoms spontaneously relax back to their original substitutional sites, and the group-III A impurity is globally stable as a shallow acceptor.

Our results indicate that it is possible to identify growth conditions for which the formation energy of substitutional acceptors is low enough and, simultaneously, the formation energy of compensating donors is high enough to achieve  $p$ -type doping. Incorporation of donor-type impurities (such as H) should, of course, also be strictly controlled. Alternatively, one could deliberately take advantage of the presence of interstitial hydrogen as a shallow donor with low formation energy. When group-III A acceptors and interstitial H are simultaneously incorporated under near-equilibrium conditions, charge neutrality pins the Fermi level at a position where compensation by any of the donor-type defects is suppressed. Additionally, the formation energy of the acceptor is significantly lowered, and hence its solubility is increased. A postgrowth anneal then removes hydrogen and activates the  $p$ -type material, a strategy that has proven successful in the case of GaN [24].

In summary, we have investigated possible causes of  $n$ -type doping and prospects for  $p$ -type doping in  $\text{SnO}_2$  based on first-principles calculations. Our results are counter to the conventional assignment of intrinsic point defects as a source of electron conductivity but entirely consistent with hydrogen acting as the unintentional donor. Most significantly, we find that  $\text{SnO}_2$  offers excellent prospects for  $p$ -type doping using In and other group-III A acceptors.

This work was supported in part by the NSF MRSEC Program under Grant No. DMR05-20415 and by the UCSB

Solid State Lighting and Energy Center. It also made use of the CNSI Computing Facility under NSF Grant No. CHE-0321368.

- 
- [1] A. L. Dawar *et al.*, *Semiconducting Transparent Thin Films* (Institute of Physics, London, 1995).
  - [2] D. C. Look *et al.*, *Phys. Status Solidi A* **201**, 2203 (2004).
  - [3] Z. M. Jarzebski and J. P. Morton, *J. Electrochem. Soc.* **123**, 299C (1976).
  - [4] M. Batzill and U. Diebold, *Prog. Surf. Sci.* **79**, 47 (2005).
  - [5] C. G. Fonstad and R. H. Rediker, *J. Appl. Phys.* **42**, 2911 (1971).
  - [6] S. Samson and C. G. Fonstad, *J. Appl. Phys.* **44**, 4618 (1973).
  - [7] M. Nagasawa and S. Shionoya, *Jpn. J. Appl. Phys.* **10**, 727 (1971).
  - [8] M. Nagasawa and S. Shionoya, *J. Phys. Soc. Jpn.* **30**, 1213 (1971).
  - [9] C. Kiliç and A. Zunger, *Phys. Rev. Lett.* **88**, 095501 (2002).
  - [10] A. Janotti and C. G. Van de Walle, *Phys. Rev. B* **76**, 165202 (2007).
  - [11] A. Janotti and C. G. Van de Walle, *Nat. Mater.* **6**, 44 (2007).
  - [12] Y. Mizokawa and S. Nakamura, *Jpn. J. Appl. Phys.* **14**, 779 (1975).
  - [13] P. D. Nola *et al.*, *J. Chem. Soc., Faraday Trans.* **89**, 3711 (1993).
  - [14] P. Türkes, C. Pluntke, and R. Helbig, *J. Phys. C* **13**, 4941 (1980).
  - [15] G. Kresse and D. Joubert, *Phys. Rev. B* **59**, 1758 (1999).
  - [16] P. E. Blöchl, *Phys. Rev. B* **50**, 17953 (1994).
  - [17] G. Kresse and J. Hafner, *Phys. Rev. B* **47**, 558 (1993).
  - [18] G. Kresse and J. Furthmüller, *Phys. Rev. B* **54**, 11 169 (1996).
  - [19] A. Janotti and C. G. Van de Walle, *Appl. Phys. Lett.* **87**, 122102 (2005).
  - [20] A. Janotti and C. G. Van de Walle, *Phys. Rev. B* **75**, 121201 (2007).
  - [21] A. Janotti, D. Segev, and C. G. Van de Walle, *Phys. Rev. B* **74**, 045202 (2006).
  - [22] H. J. Monkhorst and J. D. Pack, *Phys. Rev. B* **13**, 5188 (1976).
  - [23] W. H. Baur and A. A. Khan, *Acta Crystallogr. Sect. B* **27**, 2133 (1971).
  - [24] C. G. Van de Walle and J. Neugebauer, *J. Appl. Phys.* **95**, 3851 (2004).
  - [25] *CRC Handbook of Chemistry and Physics*, edited by D. R. Lide (CRC Press, Boca Raton, FL, 2005).
  - [26] H. L. Ma *et al.*, *Solar Energy Mater. Sol. Cells* **40**, 371 (1996).
  - [27] V. Geraldo *et al.*, *Mat. Res.* **6**, 451 (2003).
  - [28] C. Terrier *et al.*, *Thin Solid Films* **263**, 37 (1995).
  - [29] C. Kiliç and A. Zunger, *Appl. Phys. Lett.* **81**, 73 (2002).
  - [30] C. H. Park, S. B. Zhang, and S.-H. Wei, *Phys. Rev. B* **66**, 073202 (2002).
  - [31] S.-H. Wei and A. Zunger, *Phys. Rev. B* **37**, 8958 (1988).
  - [32] D. J. Chadi, *Phys. Rev. B* **59**, 15 181 (1999).